SUPPLEMENTARY MATERIAL

SUPPLEMENTARY MATERIALS & METHODS

Construction of the pKC26w-pUbiq rescue plasmid

pKC26w-pUbiq was generated from pKC26-pUbiq and pW25. First, to obtain pKC26-pUbiq, pKC26 was digested with PstI and XbaI (to remove the 10X UAS sequence) and a new MCS was introduced. The *ubiquitin-63E* promoter was cloned into MluI and KpnI sites. Subsequently, to allow insertion into any landing site, the full mini-white gene was restored. This was done by subcloning the missing mini-white gene from pW25 and mutagenizing an internal DraIII site within mini-white to allow for insertion into DraIII and SpeI sites of pKC26-pUbiq.

Immunocytochemistry

Primary antibodies used were: guinea pig anti-Magi (polyclonal directed against Magi aa 790-1202 generated for this study; 1:2000), rat anti-ASPP (1:500) (Langton et al., 2007), rabbit anti-RASSF8 (1:500) (Langton et al., 2009), rabbit anti-Bazooka (1:500) (gift from A. Wodarz; (Wodarz et al., 1999), rat anti-E-Cad (DCAD2, Developmental Studies Hybridoma Bank – DSHB; 1:25), mouse anti-Arm (N2 7A1, DSHB; 1:25), rat anti-α-Catenin (DCAT-1, DSHB; 1:25), mouse anti-β-Galactosidase (DSHB 40-1a; 1:25), mouse anti-Dlg (4F3, DSHB; 1:25), rabbit anti-aPKC (anti-PKCz C-20, SantaCruz; 1:500), rabbit anti-GFP (A6455, Molecular Probes; 1:2000), rabbit anti Cleaved Drosophila Dcp-1 (9578, Cell Signaling; 1:200).

Quantifications

Quantification of IOCs: the inter-ommatidial lattice is composed of 9 IOCs per ommatidium, six 2° and three 3° pigment cells. Each 2° pigment cell is shared by two

ommatidia and 3° pigment cell by three ommatidia. For quantification of IOCs per ommatidium, we selected complete ommatidial units and counted independently all IOCs surrounding them. Statistical relevance was obtained by performing unpaired two-tailed student t-test on raw data obtained from at least 5 experiments.

Quantification of E-Cad interruptions: 22-26h APF pupal retinas were stained with anti-E-Cad antibody. At least 7 confocal stacks spanning the entire depth of the tissues from independent retinas were taken showing mutant and wild type tissues, and flattened using the maximum projection tool in ImageJ (NIH). This ensured that no out of focus E-Cad staining was left out. Gaps in E-Cad staining were then counted in IOCs and divided by the number of IOCs to obtain the interruption per IOC index. Significance was then assessed by unpaired two-tailed student t-test.

Quantification of Baz, α-Cat, or Arm membrane levels: 22-26h APF pupal retinas were stained with the relevant antibodies and at least 7 retinas were imaged as indicated above. Using the "Freehand line selections" a line was drawn following IOC/IOC membrane as shown by an E-Cad staining. "Mean Gray Value" gave of average fluorescence intensity along the lines. At least 15 IOC/IOC membranes were quantified this way per stack and per territory (wild type (wt) vs mutant). Average fluorescence intensity for IOC/IOC membranes per image were then obtained showing substantial differences between images highlighting the importance of the clonal analysis. When levels were compared between wt and mutant tissues from the same image, and thus stained, treated, and imaged exactly the same way, membrane levels were always higher in wt. Statistical relevance was then assessed by paired two tailed student t-test using the wt/mutant tissues pairs.

SUPPLEMENTARY REFERENCES

Langton, P. F., Colombani, J., Aerne, B. L. and Tapon, N. (2007). Drosophila ASPP regulates C-terminal Src kinase activity. *Dev. Cell* 13, 773–782.

Langton, P. F., Colombani, J., Chan, E. H. Y., Wepf, A., Gstaiger, M. and Tapon, N. (2009). The dASPP-dRASSF8 complex regulates cell-cell adhesion during Drosophila retinal morphogenesis. *Curr. Biol. CB* 19, 1969–1978.

Wodarz, A., Ramrath, A., Kuchinke, U. and Knust, E. (1999). Bazooka provides an apical cue for Inscuteable localization in Drosophila neuroblasts. *Nature* 402, 544–547.

SUPPLEMENTARY FIGURES

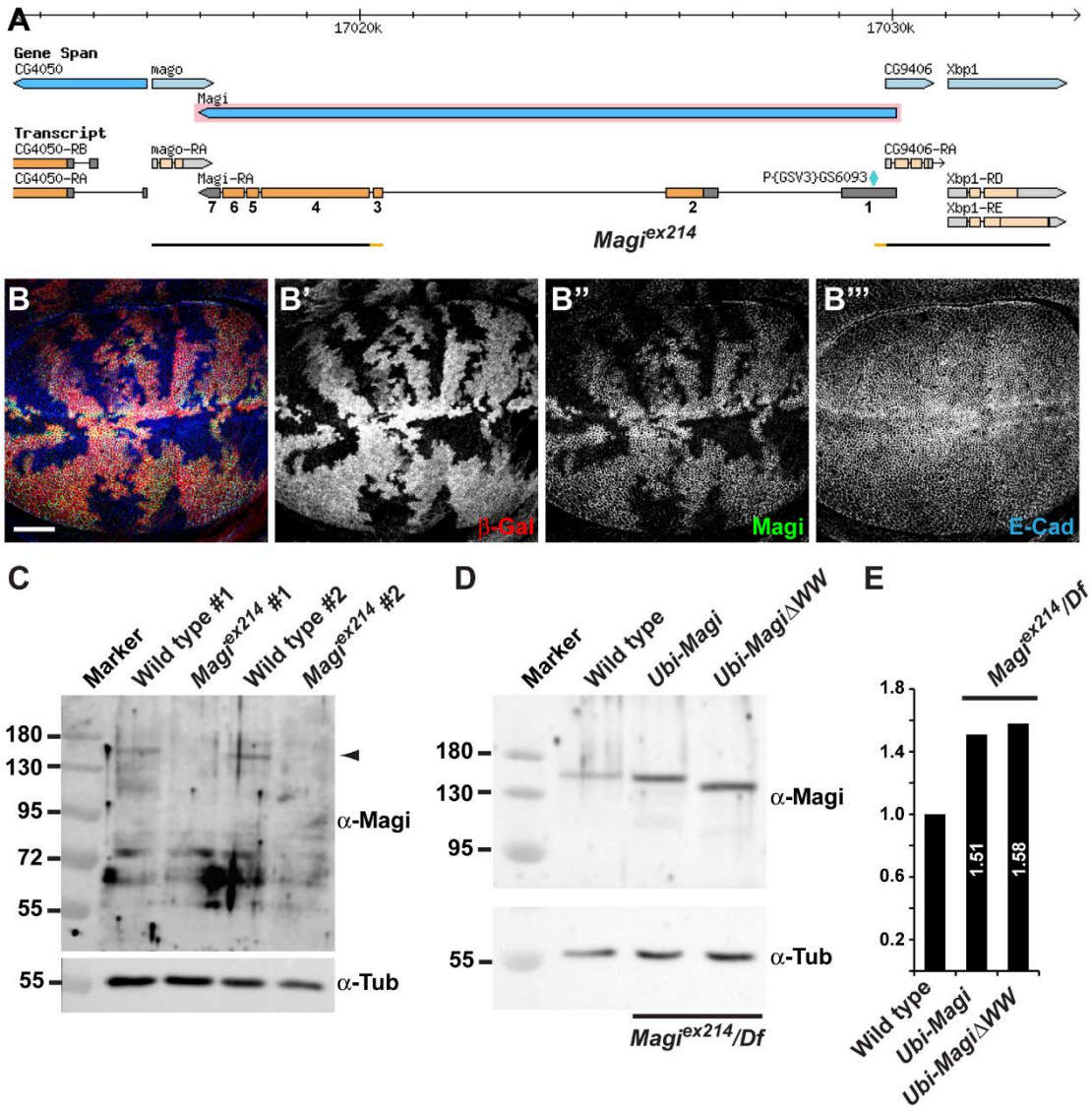

Figure S1. *Magi* expression levels.

A. *Magi* locus (adapted from Flybase GBrowse) showing novel *Magi* allele. The *Magi*^{ex214} local deletion was generated by mobilizing the viable GS6093 P element (green diamond) and mapped by PCR (absent DNA is represented by the interrupted black line; orange segments indicate regions of uncertainty). The *Magi* transcript is represented by shaded boxes (orange, coding; grey, non coding), and numbers indicate position of exons used in the text.

B. *Magi*^{ex214} mutant clones in the larval wing disc, marked by the absence of β-Galactosidase (red; B'). In mutant cells, Magi protein is totally absent (green; B"), while E-Cadherin (E-Cad; blue; B"') is unaffected. Bar, 25μm.

C. Western blot characterization of the *Magi*^{ex214} allele. Top panel: Western blot analysis using the anti-Magi antibody (α-Magi) of total protein extracts from two independent experiments (#1-2) from isolated pupal eye discs at 22-26h APF either from wild type controls or from *Magi*^{ex214} homozygotes. A band migrating slightly above 130kDa and corresponding to the predicted size for the Magi protein is present in controls but disappears in *Magi*^{ex214} mutants. An increase in other bands was not observed suggesting that other Magi fragments are not translated in the *Magi*^{ex214} mutants. Bottom panel: same membrane as in top but re-blotted with an anti-Tubulin antibody (α-Tub) used as a loading control.

D. Western blot characterization of the *Ubi-Magi* rescues. Top panel: Western blot analysis using the anti-Magi antibody (α-Magi) of total protein extracts from isolated pupal eye discs at 22-26h APF either from wild type controls or from *Magi mutants (Magi*^{ex214}*/Df(2R)Exel6072* trans-heterozygotes) carrying one copy of *Ubi-Magi* or *Ubi-MagiΔWW* transgenes. Bottom panel: same extracts as in top blotted with an anti-Tubulin antibody (α-Tub) used as a loading control.

E. Relative amounts of Magi protein from the western blot shown in B. After normalization with the Tubulin loading control, the Ubi-Magi and Ubi-MagiΔWW are expressed respectively 1.51 and 1.58 times more than the endogenous Magi protein. This shows that the Ubiquitin promoter driven Magi rescue constructs are expressed at very similar levels to the endogenous protein, and that the MagiΔWW construct is as stable as wild type Magi.

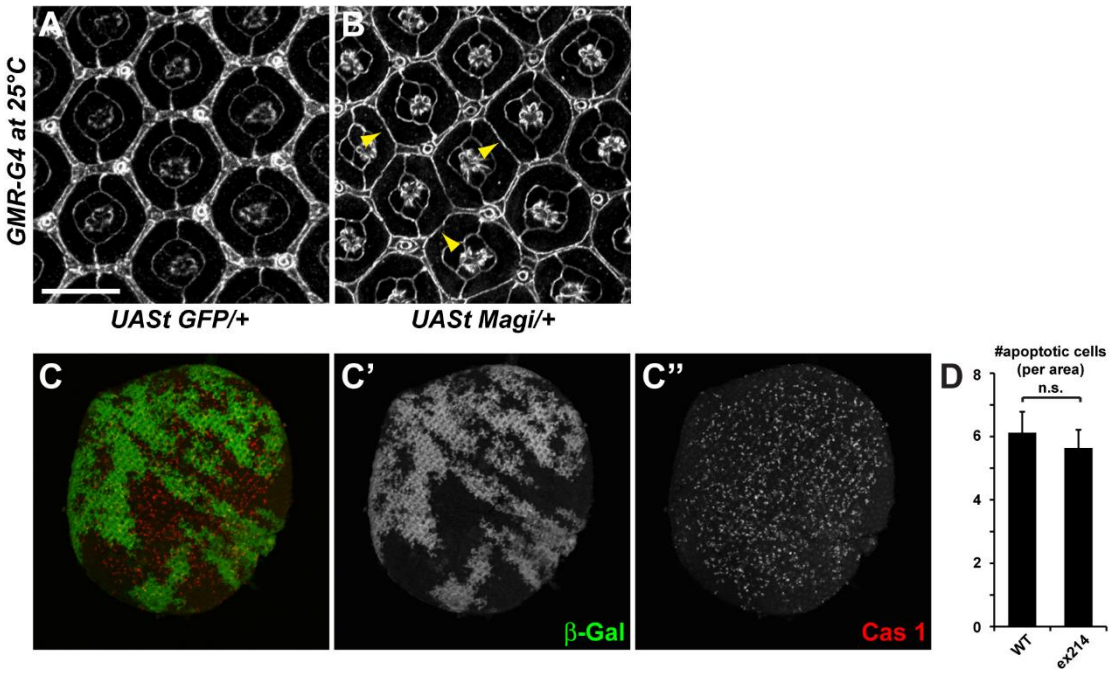

Figure S2. *Magi* and the control of IOC cell number.

A-B. Pupal eye at 44h APF stained for E-Cad (white) showing the ommatidial organization. When overexpressed under the control of the *GMR-Gal4* driver, Magi produces pupal eyes with fewer IOCs (B; yellow arrowheads) than control (A). Bar, 10 µm.

C. Whole pupal retina with Magi mutant homozygous clones marked by the absence of β-Galactosidase (green, C') and stained for activated Dcp1 (red, C").

D. Quantification of the number of activated caspase-1 puncta per arbitrary area unit in wild type (WT; β-Galactosidase positive) and Magi mutant (β-Galactosidase negative) tissues. No statistical difference was observed; sem is shown; paired two-tailed student t-test on 15 pairs of tissues; p=0.395).

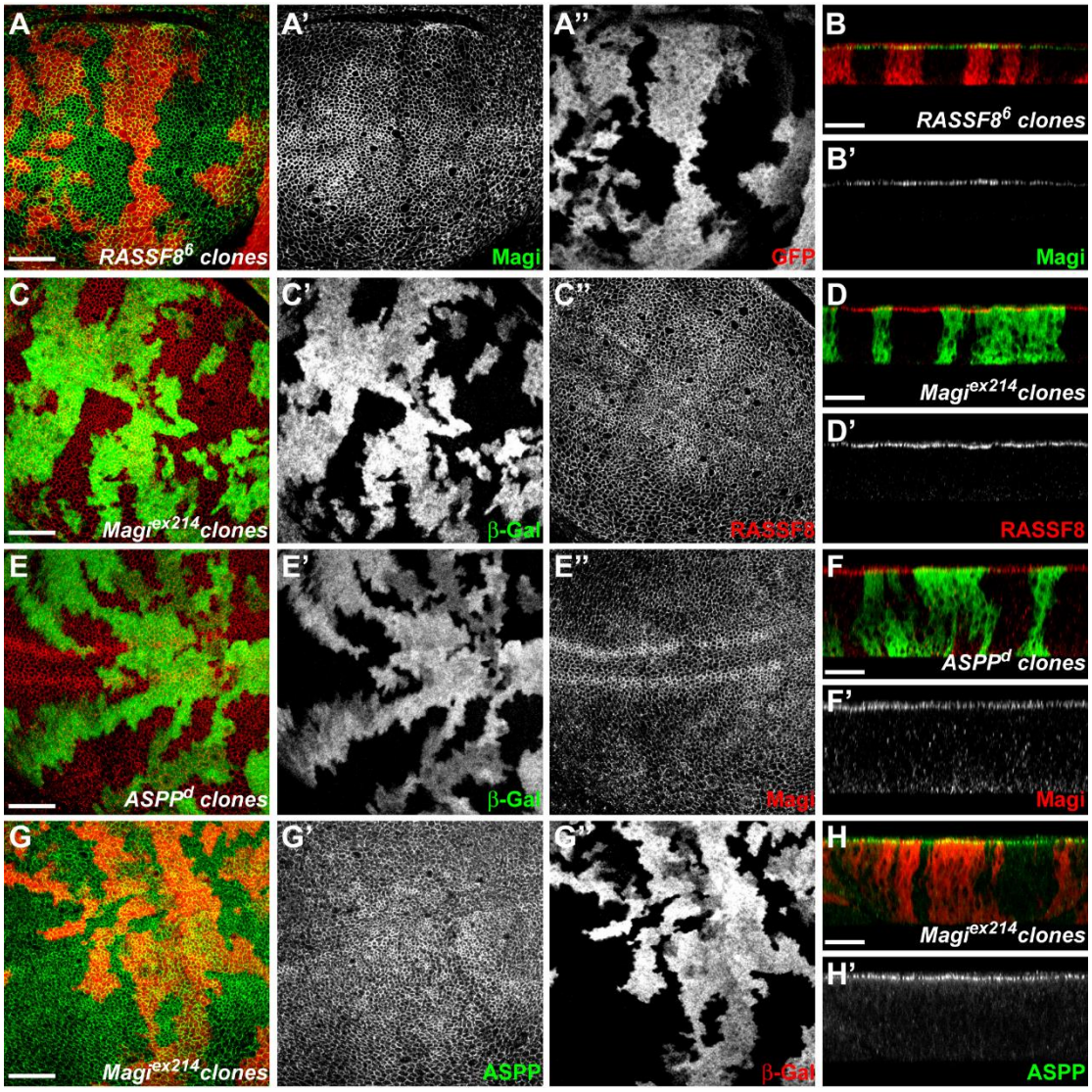

Figure S3. In 3rd instar larval wing discs, Magi and the RASSF8/ASPP complex localize independently to AJs.

A-D. Magi and RASSF8 localize independently. In *RASSF8* mutant clones (A,B), marked by the absence of GFP (red; A''), Magi protein levels and apical localization are unaffected (green; A',B'). Similarly, in *Magi* mutant clones (C,D) marked by the absence of β-Galactosidase (green; C'), RASSF8 protein levels and apical localization are unaffected (red; C''&D').

E-H. Magi and ASPP localize independently. In *ASPP* mutant clones (E,F), marked by the absence of β-Galactosidase (green; E'), Magi protein levels and apical

localization are unaffected (red; E"&F'). Similarly, in *Magi* mutant clones (G,H) marked by the absence of β-Galactosidase (red; G"), ASPP protein levels and apical localization are unaffected (green; G'&H').

xy apical (A,C,E,G) and z (B,D,F,H) confocal sections. Bars, 20 μm.

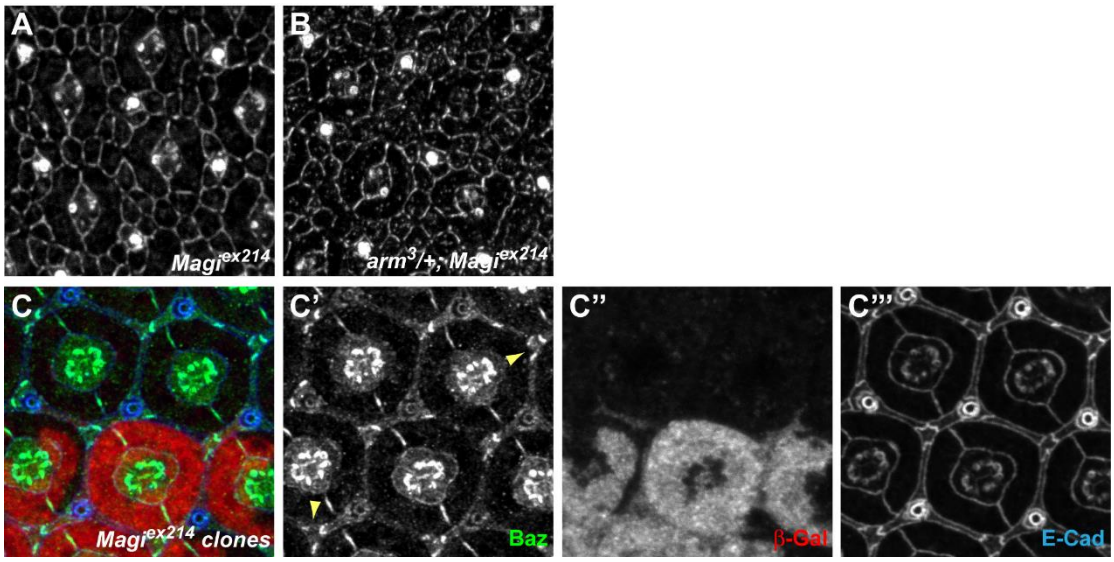

Figure S4. Magi and AJ formation.

A-B. 24h APF pupal eye discs stained for E-Cad (white; A-B). The E-Cad interruptions in *Magi*^{ex214} homozygous mutants (A) is strongly enhanced by the removal of one copy of β-catenin (*arm*^{3}/+; B).

C. At 44h APF, Baz (green; C') is localized correctly at the level of inter-IOCs membranes (yellow arrowheads), both in wild type and in *Magi* mutant clones marked by the absence of β-Galactosidase (red; C''). Membranes are highlighted with E-Cad (blue; C''').

Table S1. *Magi* mutant flies have slightly bigger wings.

Adult female wings measurement in arbitrary units (pixels) in the indicated genotypes. *Magi* mutant wings are both slightly longer and wider than controls giving rise to wings slightly bigger but of the correct shape (ratio width / length similar to control). This phenotype is different from the round wing phenotype of *RASSF8* mutants.

Table S2. Magi yeast 2-hybrid clones interacting with RASSF8.

Clones corresponding to Magi fragments and isolated in a yeast 2-hybrid screen using full length RASSF8 as bait. 3 independent clones were recovered. The minimal common regions in these clones spans from nucleotide 852 to nucleotide 1134 of Magi corresponding to amino-acids 284 to 378 around the two WW domains (see Figure 2).

Table S3. Genetic modifiers of the rough eye phenotype of overexpressed Magi.

List of mutants tested for dosage sensitivity by scoring any modification of the external adult roughness induced by UASt Magi overexpression in the eye under the control of the *GMR-Gal4* driver at 25°C.

Columns are:

- Genotype: presenting the relevant genotype. Mutants have been grouped by pathway.
- Score: indicating the level of modification. Rescues are highlighted in green; enhancements in red.
- Origin of mutation: indicates where the described mutations can be obtained; BSC = Bloomington Stock Center.
- Note: additional information available regarding the mutation used.

Table S1. *Magi* mutant flies have slightly bigger wings.

Genotype	Mean length	Stdv length	Mean width	Stdv width	Mean w/l	Stdv w/l	n
Df(2R)6072/+	782.37	16.39	560.65	12.45	0.72	0.008	19
Magi[ex214]/+	781.35	19.26	548.60	10.00	0.70	0.011	19
Magi[ex214]/Df(2R)6072	810.09	18.07	601.97	14.61	0.74	0.015	18
Magi[ex214]/Magi[ex214]	814.62	11.76	579.60	10.23	0.71	0.012	16
RASSF8[6]/RASSF8[6]	789.14	13.21	654.37	10.07	0.83	0.012	19

Conclusion: *Magi* mutant wings are both longer and larger than control, but ratio width/length (w/l) is the same, ie wings are not rounder. This phenotype is different from the *RASSF8* mutant round wing phenotype.

Table S2. Magi yeast 2-hybrid clones interacting with RASSF8.

Y2H screen using full length RASSF8 as bait.

Only clones relative to Magi are presented here.

Drosophila CG5053 (1-607) vs *Drosophila* Whole Embryo RP2 (0-12+12-24)

Clone name	Global PBS	Gene name	Start	Stop	Remarks
C-137	A	Magi CG30388	No Data	1238	Ends after the WW domains
C-213	A	Magi CG30388	519	1134	N-ter and WW domains
C-343	A	Magi CG30388	852	1239	WW domains

Summary of PBS categories
A : Very high confidence in the interaction
B : High confidence in the interaction
C : Good confidence in the interaction
D : Moderate confidence in the interaction
E : Interactions involving highly connected prey domains, warning of non-specific interaction
F : Experimentally proven technical artifacts
N/A : The PBS is a score that is automatically computed through algorithms and cannot be attributed

Table S3. Genetic modifiers of the rough eye phenotype of overexpressed Magi.

Genotype	Score	Origin	notes
PTEN			
FRT40A pten[DS189]/+	none	D. St Johnston	
FRT40A pten[C494]/+	none	D. St Johnston	
Df(2L)ED729/+	none	BSC	Deficiency for *pten*
Akt[04223]/+	none	BSC	
Df(1)BSC538/+	none	BSC	Deficiency for *Dsor1*
HIPPO PATHWAY			
ex[1]/+	none	N. Tapon	
ex[697]/+	none	N. Tapon	
kibra[del]/+	none	N. Tapon	
FRT82B sav[3]/+	slightly worse	N. Tapon	
sav[4]/+	none	N. Tapon	
FRT82B wts[X1]/+	none	N. Tapon	
wts[M541]/+	none	N. Tapon	
yki[B5]/+	none	N. Tapon	
RASSF8/ASPP			
RASSF8[4]/+	worse	N. Tapon	drives overexpression
UAS-RASSF8/+	worse	N. Tapon	drives overexpression
RASSF8[6]/+	rescue	N. Tapon	
FRT82B ASPP[d]/+	none	N. Tapon	
FRT82B ASPP[8]/+	none	N. Tapon	
Csk[J1D8]/+	none	BSC	
puc[A251.1F3]/+	none	BSC	
OTHERS			
FRT82B pyd[tamou]/+	none	A. Djiane	
FRT82B pyd[ex147]/+	none	A. Djiane	
aPKC[k06403]/+	none	BSC	